Technical Report No. 138

4853-18-T

EFFECT OF ELECTROMAGNETIC PROPAGATION ON THE MAGNETOSTATIC MODES

by

W. B. Ribbens

Approved by: B. F. Barton

for

COOLEY ELECTRONICS LABORATORY

Department of Electrical Engineering
The University of Michigan
Ann Arbor

Contract No. DA 36-039 sc-89227
Signal Corps, Department of the Army
Department of the Army Project No. 3A 99-06-001-01

June 1963

TABLE OF CONTENTS

LIST OF ILLUSTRATIONS

ABSTRACT

The second-order effect of electromagnetic propagation on the essentially static-field distribution of the magnetostatic modes of a ferromagnetic sample is obtained by an iteration-type technique. It is found that the magnetostatic potential constitutes the source in a mathematical sense for a second-order correct field distribution. The internal sample fields are investigated for a ferrite cylinder enclosed between parallel conducting plates and they are found to consist of resonant modes whose frequencies are determined from a characteristic equation. These frequencies reduce to those of the magnetostatic modes in the limit of vanishingly-small wave numbers. For a nonzero wave number the frequencies differ from the corresponding magnetostatic limits by an amount which depends on the sample shape. These resonant frequencies are size-dependent as contrasted to the size-independent magnetostatic modes. It was found that no resonant frequencies are possible above a critical value which depends on the spacing between the plates. A sample mode, whose resonant frequency is in a region forbidden to the magnetostatic modes, can exist if the sample size exceeds a critical value.

1. INTRODUCTION

A ferromagnetic sample will exhibit a number of energy storage resonances that are essentially independent of size if the sample is small compared to a wavelength. Such resonances occur in the microwave spectrum and have been explained as resonant modes of oscillation of the sample magnetization. For small samples these modes have a static field distribution which can be obtained from a scalar magnetic potential and have therefore been called magnetostatic modes (Ref. 1). However, the static fields correctly describe the actual sample fields only for infinitesimal samples. It is the purpose of the present paper to extend the static solution to include the effect of electromagnetic propagation by an iteration-type technique. Since the internal sample wavelength is many orders of magnitude greater than the lattice spacing, the effect of exchange interaction may safely be ignored. It will also be assumed that the sample shape is such that the tensor susceptibility components are independent of position in the sample.

2. THE MAGNETIC POTENTIALS AND THEIR APPROXIMATIONS

The electromagnetic fields associated with a ferromagnetic sample may be obtained from the scalar and vector magnetic potentials:

$$\bar{H} = \nabla \Phi - \frac{\partial \bar{A}}{\partial t} \tag{1a}$$

$$\bar{E} = -\frac{1}{\epsilon} \nabla \times \bar{A} \tag{1b}$$

If the Lorentz gauge condition is selected to relate these two potentials then they must satisfy similar inhomogeneous wave equations:

$$\nabla^2 \Phi + k^2 \Phi = -\nabla \cdot \bar{M} \tag{2a}$$

$$\nabla^2 \bar{A} + k^2 \bar{A} = -\mu_o \epsilon \frac{\partial \bar{M}}{\partial t} \tag{2b}$$

where $k^2 = k_i^{\,2} = \omega^2 \mu_o \epsilon$ inside sample

$= k_o^{\,2} = \omega^2 \mu_o \epsilon_o$ outside sample

and where, of course, $\bar{M} = 0$ outside the sample.

For a sample situated in free space, the potentials may be obtained formally in terms of the free space Green's function $\frac{e^{ikr}}{4\pi r}$, in the form

$$\Phi = -\frac{1}{4\pi} \int (\nabla \cdot \bar{M}) \frac{e^{ikr}}{r} \, dv' \tag{3a}$$

$$\bar{A} = -\frac{1}{4\pi} \mu_o \epsilon \int \left(\frac{\partial \bar{M}}{\partial t} \right) \frac{e^{ikr}}{r} \, dv' \tag{3b}$$

where $r = \left[\sum_{i=1}^{3} (x_i - x_i')^2 \right]^{\frac{1}{2}}$

The primed variables are the coordinates of the source points and the unprimed variables are the coordinates of the field points. These potentials may be expanded formally in a power series of (ik)

$$\Phi = -\frac{1}{4\pi} \sum_{n=0}^{\infty} \frac{(ik)^n}{n!} \int r^{n-1} (\nabla \cdot \bar{M})\, dv' \tag{4a}$$

$$\bar{A} = -\frac{1}{4\pi} \mu_o \epsilon \sum_{n=0}^{\infty} \frac{(ik)^n}{n!} \int r^{n-1} \frac{\partial \bar{M}}{\partial t}\, dv' \tag{4b}$$

Then by substituting Eqs. 4a and 4b into Eq. 1a there results:

$$4\pi \bar{H} = -\nabla \left[\int \frac{\nabla \cdot \bar{M}}{r}\, dv' + ik \int \nabla \cdot \bar{M}\, dv' + \ldots \right] - (ik)^2 \left[\int \frac{\bar{M}}{r}\, dv' + ik \int \bar{M}\, dv' + \ldots \right] \tag{5}$$

For all field points inside and on the sample the magnitude of the nth term in the first bracket is less than $[(ka)^n/n!] \left| \int (\nabla \cdot \bar{M}/r)\, dv' \right|$ where a is the largest sample dimension. If the sample is sufficiently small compared to a wavelength (i. e., $ka << 1$) then the contribution of higher-order terms will be made negligible by suitable choice of ka. A similar situation exists for the terms of the second bracket. Its leading term can be made negligible relative to the leading term of the first bracket for (ka) sufficiently small.

The lowest-order term in Eq. 5 is the so-called magnetostatic term. If $\Phi = \int (\nabla \cdot \bar{M}/4\pi r)\, dv'$ then Φ is the magnetostatic potential. It was this term that was used by Walker (Ref. 1) to describe the sample fields in the quasi static approximation, which is really valid only for zero time dependence or infinitesimal samples. The second term in the first bracket of Eq. 5 vanishes since it is the gradient of a constant. One might conclude at this point that there is no first-order term present. However the magnetization is also a function of ik so it may be expanded in a series whose coefficients are functions of position. The series for $\bar{M}$ and $\bar{H}$ may be represented as:

$$\bar{M} = \bar{M}_o + ik\, \bar{M}_1 + \ldots$$

$$\bar{H} = \bar{H}_o + (ik)\, \bar{H}_1 + \ldots \tag{6}$$

If these expressions are substituted in Eq. 5 and the first-order terms are collected there results:

$$\bar{H}_o + ik\,\bar{H}_1 = -\nabla \int \frac{\nabla \cdot (\bar{M}_o + ik\,\bar{M})}{4\pi r}\, dv' \tag{7a}$$

Then let $\bar{H}^{(1)} = \bar{H}_o + ik\,\bar{H}_1$ and $\bar{M}^{(1)} = \bar{M}_o + ik\,\bar{M}_1$ and $\Phi^{(1)} = \int (\nabla \cdot \bar{M}^{(1)}/4\pi r)\, dv'$ where the superscript represents a truncated series correct to first order. It is seen that $H^{(1)} = \nabla\Phi^{(1)}$, but $\nabla \cdot \bar{B} = \mu_o [\nabla \cdot (\bar{M} + \bar{H})] = 0$ and $\bar{M}$ is related to $\bar{H}$ by the susceptibility tensor (see Eq. 15): $\bar{M}^{(1)} = (X)\,\bar{H}^{(1)} = (X)\,\nabla\Phi^{(1)}$ so:

$$\nabla^2 \Phi^{(1)} = -\nabla \cdot [(X)\,\nabla\Phi^{(1)}] = -K\,\nabla_t{}^2 \Phi^{(1)} \tag{7b}$$

where the subscript t refers to transverse coordinates and where K is the diagonal component of (X). The above equation is the same as that used by Walker to characterize the magnetostatic modes. Therefore the magnetostatic mode approximation can be used to describe the fields inside a ferromagnetic sample correct to the first-order effects of electromagnetic propagation.

2.1 The Second-Order Magnetic Field

If $\Phi^{(2)}$ and $\bar{H}^{(2)}$ represent respectively the scalar potential and magnetic field correct to second order then:

$$\bar{H}^{(2)} = \nabla\Phi^{(2)} + \frac{k^2}{4\pi} \int \frac{\bar{M}_o}{r}\, dv' \tag{8}$$

It is possible to know $\Phi^{(2)}$ correctly only if $\bar{M}$ is known to second order. The magnetization is related to $\bar{H}$ through the susceptibility tensor and because $\nabla \cdot \bar{B}$ must vanish a pair of self-consistent equations (correct to second order) can be solved simultaneously to determine $\Phi^{(2)}$:

$$\bar{M}^{(2)} = (X)\left[\nabla\Phi^{(2)} + \frac{k^2}{4\pi} \int \frac{\bar{M}_o}{r}\, dv'\right] \tag{9}$$

and

$$\nabla^2 \Phi^{(2)} + k^2 \Phi^{(2)} = -\nabla \cdot \bar{M}^{(2)} \tag{10}$$

Combining these equations produces an expression for $\Phi^{(2)}$:

$$(1 + K)\,\nabla_t^2 \Phi^{(2)} + \frac{\partial^2 \Phi^{(2)}}{\partial z^2} + k_i^2\,\Phi^{(2)} = -\frac{k_i^2}{4\pi}\,\nabla \cdot \left[(X) \int \frac{\bar{M}_o}{r}\, dv'\right] \tag{11}$$

inside the sample and:

$$\nabla^2 \Phi^{(2)} + k_o^2\,\Phi^{(2)} = 0 \text{ outside the sample} \tag{12}$$

The boundary conditions are the continuity of potential and the normal component of flux density.

The nonhomogeneous equation (11) can be solved by use of the appropriate Green's function. The source for this equation $\rho = (-k_i^2/4\pi r)\,\nabla \cdot [(X)\,\bar{A}_o]$ is derived from the magnetostatic approximation which will be presumed known. For the free-space situation $\bar{A}_o = \int (\bar{M}_o)\,(4\pi r)^{-1}\, dv'$ so the differential equation for $\bar{A}_o$ is:

$$\nabla^2\,\bar{A}_o = -\,\bar{M}_o$$

This equation must be solved using the correct Green's function for the geometry in which $\bar{A}_o$ must satisfy the same homogeneous boundary conditions as $\bar{H}$. By Green's identity the solution to Eq. 11 will be

$$\Phi_i^{(2)} = \int_{\text{sample}} G\,\rho_m\, dv' - \int_{\text{surf. of sample}} \left[\Phi^{(2)}\,\nabla_n G - G\,\nabla_n \Phi^{(2)}\right] da'$$

where G is the Green's function and where $\rho_m = 4\pi\,\rho(1+K)^{-1}$. The potential at the sample surface is known $\left[\text{i.e., } \Phi_{in}^{(2)}\,\big|_{\text{surf.}} = \Phi_{out}^{(2)}\,\big|_{\text{surf.}}\right]$ but the normal gradient of $\Phi_i^{(2)}$ is not known there, so the Green's function will be chosen to vanish on the surface. Thus the Green's function will satisfy:

$$\nabla_t^2 G + \frac{1}{1+K}\,(\nabla_z^2 G + k_i^2 G) = -\,\delta(r - r')\,\delta(\phi - \phi')\,\delta(z - z') \tag{13a}$$

$$G = 0 \text{ at sample surface} \tag{13b}$$

One of the boundary conditions has already been used so the remaining condition of continuity of normal flux density must be applied. Neglecting the permeability of free space which is a constant factor this boundary condition may be written as follows:

$$\left(\frac{\partial \Phi^{(2)}_{out}}{\partial n} + k_o^2 \, \bar{\bar{A}}_{o_{out}} \cdot \hat{n} \right) \Bigg|_{surf.} =$$

$$\left\{ (1+K) \left[\frac{\partial \Phi^{(2)}_{in}}{\partial n} + k_i^2 \, \bar{A}_{o_{in}} \cdot \hat{n} \right] + i\nu \left[\frac{\partial}{\partial \tau} \Phi^{(2)}_{in} + k_i^2 \, \bar{A}_{o_{in}} \cdot \hat{\tau} \right] \right\} \Bigg|_{surf.} \qquad (14a)$$

where n is the coordinate normal to the surface, τ is the coordinate tangential to the surface and $\hat{n}$ and $\hat{\tau}$ are unit vectors in the respective coordinate directions. Equation 14 contains one undetermined constant. This constant is the ratio of the magnitudes of the scalar potentials outside to inside the sample. If ρ_m were an independent source (i. e., determined by external devices) then the above constant would be determined by Eq. 14. However, ρ_m depends on the coefficient of $\Phi^{(2)}$ so it is merely a source in the mathematical sense that is derived from the magnetostatic approximation. There is an additional condition to be applied in this problem namely that the magnetostatic approximation must still be valid. In the limit of vanishing k the external potential must be equal to the internal magnetostatic potential at the sample surface. Thus the limit:

$$\lim_{k \to 0} \left[\Phi^{(2)}_{out} \right] \Bigg|_{\substack{\text{sample} \\ \text{surface}}} = \Phi_{o_{in}} \Bigg|_{\substack{\text{sample} \\ \text{surface}}} \qquad (14b)$$

determines the constant in Eq. 14a. When this value is substituted into Eq. 14a the latter becomes the characteristic equation of the sample modes. Equation 14a then will have roots only for discrete values of the parameters K and ν which depend on frequency and are not independent.

For any given sample size, as k approaches zero, Eq. 14a approaches the characteristic equation of the magnetostatic modes, but letting $k \to 0$ for a fixed sample size is equivalent to letting the wavelength get arbitrarily large compared to the maximum sample dimension. The magnetostatic approximation is valid for this situation. Thus the effect of electromagnetic propagation on the resonant frequencies of the magnetostatic modes may be demonstrated by independently varying the parameter k. In order to illustrate the details of this effect a specific example will now be presented.

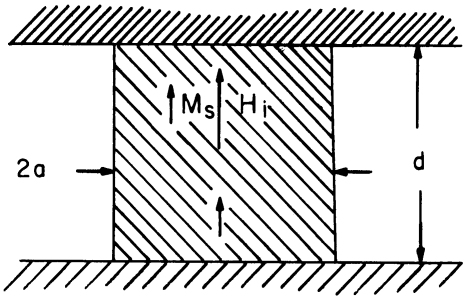

Fig. 1. A ferrite cylinder is enclosed between a pair of infinite parallel perfectly conducting plates. The sample is saturated axially by H.

2.2 An Example

Consider the case of the circularly cylindrical ferrite rod enclosed between a pair of infinite parallel conducting plates with its axis normal to the plates (see Fig. 1). This problem is particularly convenient because it is separable and because the boundary conditions are easily applied. The sample is saturated axially by a dc magnetic field. A circularly cylindrical coordinate system is chosen with its axis along the sample axis and with its origin on one of the plates. The susceptibility is a tensor:

$$(X) = \begin{bmatrix} K & i\nu \\ -i\nu & K \end{bmatrix} \tag{15}$$

where K and ν are as defined in Ref. 1 and independent of position in the sample. The tensor elements will not be independent of position for a sample shape which is not an ellipsoid of revolution but by the method of Appendix II such independence is possible. Because the sample is saturated axially the boundary conditions at the plates are the vanishing of the normal component of magnetic field. The boundary conditions at the lateral surface are the continuity of potential and normal flux density.

Because of the boundary conditions on the potential the conditions on the Green's function for the scalar potential will be: $G = 0$ on the lateral surface (i. e., $r = a$) and $\nabla_n G = 0$ at the ends of the sample. In this case the solution to Eq. 11 becomes by Green's identity:

$$\Phi_{in}^{(2)} = \int_{\text{sample}} G\,\rho_m\,dv' - \int_{\substack{\text{lateral}\\ \text{surface}}} \Phi_{out}^{(2)}\,\nabla_n G\,da' \qquad (16)$$

where $\rho_m = k_i^2\,(1+K)^{-1}\,\nabla \cdot [(X) \cdot \bar{A}_o]$

The homogeneous boundary condition on the metal plates will mean that the scalar potentials inside and outside the sample must vary as $\cos \beta_m z$, where $\beta_m = \frac{m\pi}{d}$ and where d = length of the sample and also the spacing between the plates.

The external potential may be written down at once from Eq. 12:

$$\Phi_{out}^{(2)} = B\,K_n(\alpha_1 r)\,e^{\pm\, in\,\phi}\cos \beta_m z \qquad (17)$$

where $\alpha_1 = (\beta_m^2 - k_o^2)^{\frac{1}{2}}$ and K_n is the modified Bessel function of the second kind.

The Green's function for this physical arrangement is:

$$G = -\frac{J_n(\alpha_2 r')\,C_n(\alpha_2 r)\,e^{\pm\, in|\phi-\phi'|}\cos \beta_m z \cos \beta_m z'}{\alpha_2 \pi\, da\, C_n'(\alpha_2 a)\, J_n(\alpha_2 a)} \qquad r \geqq r'$$

$$G = -\frac{J_n(\alpha_2 r)\,C_n(\alpha_2 r')\,e^{\pm\, in|\phi-\phi'|}\cos \beta_m z \cos \beta_m z'}{\alpha_2 \pi\, da\, C_n'(\alpha_2 a)\, J_n(\alpha_2 a)} \qquad r \leqq r' \qquad (18)$$

where $C_n(\alpha_2 r) = J_n(\alpha_2 r) + \Gamma_n N_n(\alpha_2 r)$ and where $C_n(\alpha_2 a) = 0$ determines Γ_n and where $\alpha_2 = \left(\frac{k_i^2 - \beta_m^2}{1+K}\right)^{\frac{1}{2}}$ and a = sample radius.

Using this Green's function in the surface integral of Eq. 16 the latter becomes:

$$\Phi^{(2)} = \int G\,\rho_m\,dv' + B\,\frac{K_n(\alpha_1 a)\,J_n(\alpha_2 r)}{J_n(\alpha_2 a)}\,e^{\pm\, in\,\phi}\cos \beta_m z \qquad (19)$$

To determine ρ_m the equation $\nabla^2 \bar{A}_o = -\bar{M}_o$ must be solved. This may be accomplished by means of another Green's function which satisfies $\nabla^2 G_o = -\delta(r - r')\,\delta(\phi - \phi')\,\delta(z - z')$. It should be noted that $k^2\,\bar{A}_o$ is the second-order contribution to the magnetic field due to the vector potential. This quantity will be used not only to obtain ρ_m but to write the boundary condition of the normal flux density. Using Green's identity:

$$A_{o_i} = \int_{\text{all space}} G_o M_{o_i} \, dv' + \text{a surface integral} \tag{20}$$

for each component of $\bar{A}_o$. The surface integral will be taken along the plates and across a lateral surface at infinity. Because $\bar{M}_o$ contains only transverse components $\bar{A}_o$ will contain only transverse components. The normal derivative of the transverse components of $\bar{A}_o$ must vanish at the plates so that if $\nabla_n G_o = 0$ at the plate then the surface integral is identically zero. This Green's function G_o then becomes:

$$G_o = \frac{K_n(\beta_m r') \, I_n(\beta_m r) \, e^{\pm in|\phi-\phi'|} \cos \beta_m z \cos \beta_m z'}{\beta_m \pi \, da \, [I_n'(\beta_m a) \, K_n(\beta_m a) - I_n(\beta_m a) \, K_n'(\beta_m a)]} \qquad r \leqq r'$$

$$G_o = \frac{K_n(\beta_m r) \, I_n(\beta_m r') \, e^{\pm in|\phi-\phi'|} \cos \beta_m z \cos \beta_m z'}{\beta_m \pi \, da \, [I_n'(\beta_m a) \, K_n(\beta_m a) - I_n(\beta_m a) \, K_n'(\beta_m a)]} \qquad r \geqq r' \tag{21}$$

The quantity $\bar{M}_o$ is the magnetostatic approximation to the magnetization:

$$\bar{M}_o = \left(K \frac{\partial \Phi_o}{\partial r} + \frac{i\nu}{r} \frac{\partial \Phi_o}{\partial \phi} \right) \hat{r} + \left(-i\nu \frac{\partial \Phi_o}{\partial r} + \frac{K}{r} \frac{\partial \Phi_o}{\partial \phi} \right) \hat{\phi} \tag{22}$$

where Φ_o is the magnetostatic potential which was determined in a previous paper (Ref. 3):

$$\Phi_o = I_n \left(\frac{\beta_m r}{\sqrt{1+K}} \right) e^{\pm in\phi} \cos \beta_m z \tag{23}$$

Here, a unity coefficient has been arbitrarily selected without loss of generality. Using the component values of $\bar{M}_o$, as obtained from Eqs. 22 and 23, and using the Green's function G_o, the components of $\bar{A}_o$ may be obtained:

$$A_{ro} = F(r, K, \nu) \, e^{\pm in\phi} \cos \beta_m z$$

$$A_{\phi o} = i \, G(r, K, \nu) \, e^{\pm in\phi} \cos \beta_m z$$

where F and G are real functions (see Appendix I). Using these components of $\bar{A}_o$ the source ρ_m may be obtained:

$$\rho_m = H(r, K, \nu) \, e^{\pm in\phi} \cos \beta_m z$$

where H is also a real valued function of r, K, ν and is listed in Appendix I. Using this ρ_m and the G from Eq. 22 it is possible to write Eq. 19 as:

$$\Phi^{(2)} = H_1(r, K, \nu) + B \frac{K_n(\alpha_1 a)\, J_n(\alpha_2 r)}{J_n(\alpha_2 a)} \; e^{\pm in\phi} \cos \beta_m z$$

where H_1 is a real function of r, K, ν (see Appendix I). If these quantities are substituted in Eq. 14a it becomes for this problem (neglecting common factors):

$$\alpha_1 B K_n'(\alpha_1 a) + k_o^2 F_o(a, K, \nu) = (1+K) \left\{ k_i^2 \frac{\partial}{\partial a} H_1(a, K, \nu) + \alpha_2 B K_n(\alpha_1 a) \frac{J_n'(\alpha_2 a)}{J_n(\alpha_2 a)} + k_i^2 F_i(a, K, \nu) \right\} -$$

$$\nu \left\{ \pm \frac{n}{a} \left[k_i^2 \frac{H_1(a, K, \nu)}{1+K} + B K_n(\alpha_1 a) \right] + k_i^2 G_i(a, K, \nu) \right\} \qquad (24)$$

where F_o, F_i and G_i are the functions F and G outside and inside the sample surface respectively. F_o, F_i, G_i and H_1 are real and appear in Appendix I. The value of B as determined from Eq. 14b is:

$$B = \frac{K_n\left[(\beta_m a)(1+K)^{-1/2}\right]}{K_n(\beta_m a)}$$

Using this value for B the characteristic equation of the sample modes may be written:

$$\alpha_1 \frac{K_n'(\alpha_1 a)}{K_n(\alpha_1 a)} - (1+K)\, \alpha_2 \frac{J_n'(\alpha_2 a)}{J_n(\alpha_2 a)} \pm \frac{n\nu}{a} = \frac{K_n(\beta_m a)\, H_2(a, K, \nu)}{K_n(\alpha_1 a)\, I_n\left[\beta_m a (1+K)^{-1/2}\right]} \qquad (25)$$

where H_2 is defined in Appendix I.

The roots of the characteristic equation (25) may be obtained graphically by defining $y = a\sqrt{(k_i^2 - \beta_m^2)(1+K)^{-1}}$ as the independent variable and plotting both sides of Eq. 25 as a function of y for each n and m. The two resulting graphs for each n and m will intersect in an infinite number of points ($y_{nm\ell}$) which are the roots of Eq. 25. A similar technique was used (Ref. 3) to obtain the roots for the magnetostatic approximation by defining $X = \beta_m a\sqrt{(1+K)^{-1}}$ and obtaining $X_{nm\ell}$. From the form of Eq. 25 it can be seen that it reduces to the characteristic equation of magnetostatic modes (Ref. 3) for $k_i = 0$. The

fact that $y = i X$ for $k_i = 0$ is only a consequence of the particular form in which the internal expansion modes were written and the significant relation is that $|y| = |X|$ for $k_i = 0$.

From the sets of roots $X_{nm\ell}$ and $y_{nm\ell}$ the normal expansion modes and hence internal fields are specified for either the magnetostatic case or the second order solution. Thus a more careful investigation of these roots will constitute a specification of the salient features of the effect of propagation on the magnetostatic approximation. There are five such features:

(1) The roots specify a set of corresponding resonant frequencies $\omega_{nm\ell}$;

(2) There is a frequency above which the resonant frequencies are complex;

(3) The values of $y_{nm\ell}$ are shifted from $X_{nm\ell}$ for $k_i > 0$ by an amount which depends on the sample shape;

(4) The more exact values for $\omega_{nm\ell}$ are size dependent whereas the magnetostatic values are size independent;

(5) Sample modes are possible in a frequency region in which magnetostatic modes cannot exist.

2.3 Resonant Frequencies

Because k, K and ν are each functions of frequency then y is also a function of frequency and discrete values for y correspond to discrete frequencies ($\omega_{nm\ell}$). Physically the values of K and ν are determined from the frequency of oscillation of the assembly of magnetic moments which produce the magnetization of the sample. Therefore the normal expansion modes each correspond to an oscillation of the sample magnetization. Energy can be coupled into the sample from external microwave circuitry at each of these frequencies so that they may be considered sample resonances. In actual samples there will be losses so that a measureable Q will exist at each sample resonance. These resonances have been observed experimentally and their characteristics noted (Ref. 4).

2.4 The Effect of Imaginary Parameters

The resonant frequencies will be real for all frequencies such that α_1 is real. However, when α_1 is imaginary the characteristic equation will contain a ratio of Hankel

functions which is in general complex. The roots in this case will be complex and cannot correspond to resonant sample frequencies. For all $\omega < \omega_c = \beta_m(\mu_o\epsilon_o)^{-1/2}$ the parameter α_1 will be real and resonant sample modes can exist. It is interesting to note that for α_1 imaginary the external potential is proportional to $H_n^{(1)}(|\alpha_1|r)$ which in the present convention represents an outgoing wave. Thus the sample modes exist in a frequency region in which the external fields are evanescent.

It is also possible for α_2 to have imaginary values but the effect of this on the roots of Eq. 25 is much less severe. The internal potential is proportional to $J_n(\alpha_2 r)$ and this function enters the characteristic equation as $\alpha_2 J_n'(\alpha_2 a)/J_n(\alpha_2 a)$ which is a real ratio whether α_2 is real or imaginary. Therefore Eq. 25 has real roots independently of whether α_2 is real or imaginary.

2.5 Shift in Resonant Frequencies

It has been shown that $y = iX$ for $k = 0$ and that the resonant frequencies derived from y reduce to those of the magnetostatic modes for $k = 0$. This corresponds to an infinite wavelength which is physically incorrect for a time dependent field. However, it has been demonstrated for samples sufficiently small compared to a wavelength that k may be neglected relative to terms of the order of $1/a$ for a first-order approximation. Letting $k = 0$ in the second order solution is a somewhat artificial means of representing this situation. If k is replaced by ηk in Eq. 25 and η varied from zero to unity, the effect of propagation on the roots of the characteristic equation can be demonstrated. This was done and it was found that for the roots corresponding to real α_2 the roots shift by a larger amount for large α than for small α where α is the aspect ratio of the sample (a/d). This means that the magnetostatic approximation is better for long thin cylinders than for flat thin disks, provided the maximum size is small compared to a wavelength in both cases.

The latter phenomenon may be explained by comparing the nature of the magnetostatic solution with the second order solution. In both cases, the axial components of the scalar potential consist of standing waves, which is also true for the exact solution. The approximation has been introduced in the radial component so the approximate solution is better for small radii (thin cylinders) than large radii (flat disks), since (ka) is smaller for the former than for the latter. Thus the magnetostatic approximation is better for thin

cylinders than flat disks. This situation is not fundamental to the magnetostatic approximation but may be attributed to the artificiality of the homogeneous boundary condition at the plates for the configuration of the example (Ref. 3).

2.6 Size Dependence of Sample Modes

It was demonstrated in Ref. 3 that the resonant frequencies of the magnetostatic modes are independent of sample size but depend largely on sample shape. This result was arrived at because the sample dimensions enter the characteristic equation for the magnetostatic modes only in the sample aspect ratio. However it is not possible to specify Eq. 25 entirely in terms of this ratio. Rather it is necessary to know the actual radius and length of the sample to compute $y_{nm\ell}$. Therefore the resonant frequencies, which are specified by $y_{nm\ell}$, depend on the actual sample size, a fact which is consistent with experiment (Ref. 4).

2.7 Resonance Outside the Frequency Region of the Magnetostatic Modes

From the literature (Ref. 5) it has been shown that magnetostatic modes can be classified as volume modes or surface modes depending upon whether $1 + K$ is positive or negative. It has also been shown (Ref. 6) that magnetostatic modes cannot exist in the frequency region $\omega < \gamma H_i$ where H_i is the internal biasing magnetic field and γ is the gyromagnetic ratio. However, the more exact solution shows that modes can exist in this region provided the sample size exceeds a certain minimum. This can be shown with reference to the definition of y and with the observation that $K > 0$ when $\omega < \gamma H_i$:

$$\left|y\right| = \left| a\sqrt{\frac{k_i^2 - \beta_m^2}{1 + K}} \right|$$

so
$$\left|\sqrt{1 + K}\right| = \frac{a\left|\sqrt{k_i^2 - \beta_m^2}\right|}{\left|y\right|} > 1 \qquad \text{for } \omega < \gamma H_i$$

then
$$a > \frac{y_{nm\ell}}{\left|\sqrt{k_i^2 - \beta_m^2}\right|} \qquad \text{for } \omega_{nm\ell} < \gamma H_i .$$

However for samples of this size $(a\, k_i) > y_{nm\ell} \left| \sqrt{(1 - \beta_m^2/k_i^2)^{-1}} \right|$ which is not necessarily small compared to unity and so the predictions based on the second-order solution are not valid. Nevertheless the exact solution would involve the same Green's function for the scalar

potential. Even though the latter is not sufficient by itself for writing the boundary conditions it would form a part of the final characteristic equation and would therefore determine at least in part the resonant frequencies of sample modes. The functional form of the potential would still be proportional to $J_n \left[a\sqrt{(k_i^2 - \beta_m^2)\,(1+K)^{-1}} \right]$ in the characteristic equation and so the definition of y could be used for a graphical solution for the roots. Thus there would be a set of values $y_{nm\ell} = a\sqrt{(k_i^2 - \beta_m^2)\,(1+K)^{-1}}$ which would determine the sample resonant frequencies. Then the criterion that $1 + K > 1$ for a frequency less than γH_i would again predict a minimum sample size for such a result. There is nothing at all new in this fact since for large samples a cavity-type resonance must be observed in which the sample modes are intimately related to the surrounding microwave structure.

If $a_c = y_{nm\ell}(k_i^2 - \beta_m^2)^{1\,2}$ is defined as the critical sample size then resonance below the region of magnetostatic modes is possible for all samples exceeding this size. This critical sample has a minimum for each root of the characteristic equation as a function of frequency. The frequency for the minimum sample size is determined by λ, the ratio of the saturation magnetization to the internal biasing field and is $\omega_{min} = \gamma H_i \sqrt{(1+\lambda) - (\lambda+\lambda^2)^{\frac{1}{2}}}$ It is not possible to compute the actual critical size without first obtaining the roots of the exact characteristic equation but the prediction that resonances occur below γH_i was based only on the form of the exact characteristic equation and useful features of its roots.

3. CONCLUSIONS

The magnetostatic mode field distribution is the zero-order approximation to the field in terms of ka where a is a maximum outside sample dimension. The second-order solution has shown that:

(1) The field distribution consists of resonant modes which reduce to the magnetostatic modes for $k = 0$;

(2) The corrections to the resonant frequencies of the magnetostatic modes depend on the sample shape;

(3) The resonant frequencies were found to be size dependent as contrasted to the size independent magnetostatic resonances;

(4) Resonant frequencies are complex above a critical frequency. The form of the exact solution has shown that: a sample resonance can occur outside the region to which the magnetostatic resonances are confined if the sample exceeds a critical minimum.

APPENDIX I

$$F_o = \frac{d}{am\pi d_n} \left\{ K_n(\beta_m r) \left[(K \mp \nu)n \int_o^a I_n(\beta_m r') I_n\left(\frac{\beta_m r'}{\sqrt{1+K}} \right) dr' + \frac{K\beta_m}{\sqrt{1+K}} \int_o^a I_n(\beta_m r') I_{n+1} \left(\frac{\beta_m r'}{\sqrt{1+K}} \right) r' \, dr' \right] \right\}$$

$$F_i = \frac{d}{am\pi d_n} \left\{ K_n(\beta_m r) \left[(K \mp \nu)n \int_o^r I_n(\beta_m r') I_n\left(\frac{\beta_m r'}{\sqrt{1+K}} \right) dr' \right] + \left[\frac{K\beta_m}{\sqrt{1+K}} \int_o^r I_n(\beta_m r') I_{n+1} \left(\frac{\beta_m r'}{\sqrt{1+K}} \right) r' \, dr' \right] + I_n(\beta_m r) \left[(K \mp \nu)n \int_r^a K_n(\beta_m r') I_n\left(\frac{\beta_m r'}{\sqrt{1+K}} \right) \int_r^a K_n(\beta_m r') I_n\left(\frac{\beta_m r'}{\sqrt{1+K}} \right) r' \, dr' \right] \right\}$$

$$G_i = \frac{d}{am\pi d_n} \left\{ K_n(\beta_m r) \left[(\mp K - \nu)n \int_o^r I_n(\beta_m r') I_n\left(\frac{\beta_m r'}{\sqrt{1+K}} \right) dr' - \frac{\nu \beta_m}{\sqrt{1+K}} \int_o^r I_n(\beta_m r') I_{n+1} \left(\frac{\beta_m r'}{\sqrt{1+K}} \right) r' \, dr' \right] + I_n(\beta_m r) \left[(\mp K - \nu)n \int_o^a K_n(\beta_m r') I_n\left(\frac{\beta_m r'}{\sqrt{1+K}} \right) dr - \frac{\nu \beta_m}{\sqrt{1+K}} \int_r^a K_n(\beta_m r') I_{n+1} \left(\frac{\beta_m r'}{\sqrt{1+K}} \right) r' \, dr' \right] \right\}$$

$$H_1(a, K, \nu) = \frac{C_n(\alpha_2 a)}{ad\,\alpha_2\, C_n'(\alpha_2 a)\, J_n(\alpha_2 a)} \int_o^a J_n(\alpha_2 r)\, \rho_m \, r dr$$

$$H_2(a,K,\nu) = (1+K)\left[\frac{1}{aJ_n(\alpha_2 a)}\int_0^a J_n(\alpha_2 r)\,\rho_m(r)\,r\,dr + k_i^2\,F_i(a,K)\right] -$$

$$\nu k_i^2\,G_i(a,K) - k_o^2\,K_n(m\pi\alpha)\,H(K)$$

where

$$\rho_m = \frac{k_i^2}{1+K}\left\{\frac{\partial}{\partial r}\left[K\,F_i(r,K) - kG_i(r,K)\right] \pm \frac{n}{a}\left[F_i(r,K) - kG_i(r,K)\right]\right\}$$

$$H(k) = \frac{d}{m\pi a d_n}\left[(K \mp \nu)n\int_0^a I_n(\beta_m r')\,I_n\left(\frac{\beta_m r'}{\sqrt{1+K}}\right)dr' + \frac{K\beta_m}{\sqrt{1+K}}\int_0^a I_n(\beta_m r')\,I_{n+1}\left(\frac{\beta_m r'}{\sqrt{1+K}}\right)r'\,dr'\right]$$

$$d_n = I_n'(\beta_m a)\,K_n(\beta_m a) - I_n(\beta_m a)\,K_n'(\beta_m a)$$

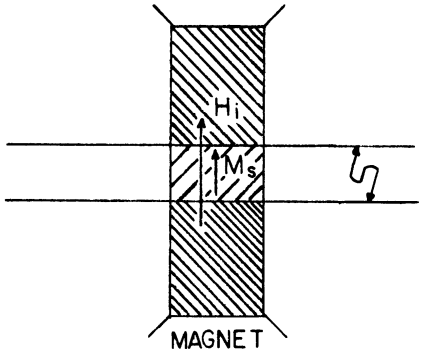

Fig. 2. The section of the ferromagnetic cylinder between plates will support a very uniform internal field.

APPENDIX II

The requirement that the susceptibility tensor components be independent of position in the sample effectively demands that the internal dc magnetic field be uniform. Clearly this cannot be the case if the sample is placed in the uniform field of a magnet. The demagnetizing field will be highly nonuniform for such an arrangement. However it is possible to maintain a uniform internal field in the following physical arrangement (see Fig. 2): from a long cylinder of the material desired and of the diameter of interest, cut a right section of the length desired; place this section in a strip line of spacing equal to the section length; obtain two more cuts from the original cylinder which are each long compared with the spacing of the strip line and place them, one on either side of the strip line coaxial with the section included in it; magnetize to saturation along the common axis. The dc field in the section between the strip line plates will be uniform since it is in the middle portion of a long ferromagnetic cylinder. The microwave energy will be contained in the strip line and so the section so included will be the equivalent of that picture in Fig. 1 in which the internal dc field is uniform.

REFERENCES

1. L. R. Walker, "Magnetostatic Modes in Ferromagnetic Resonance," Phys. Rev., Vol. 105, p. 390.

2. L. R. Walker, loc. cit.

3. W. B. Ribbens, "Note on the Size Independence of Magnetostatic Modes," Proc. IRE, Vol. 51, February 1963, p. 394.

4. L. R. White and I. H. Solt, "Multiple Ferromagnetic Resonance in Ferrite Spheres," Phys. Rev., Vol. 104, October 1956, p. 56.

5. R. I. Joseph and E. Schlömann, "Theory of Magnetostatic Modes in Long, Axially Magnetized Cylinders," J. Appl. Phys., Vol. 32, June 1961, p. 1001.

6. L. R. Walker, loc. cit.

DISTRIBUTION LIST

Copy No.	
1-2	Commanding Officer, U. S. Army Electronics Research and Development Laboratory, Fort Monmouth, New Jersey, ATTN: Senior Scientist, Electronic Warfare Division
3	Commanding General, U. S. Army Electronic Proving Ground, Fort Huachuca, Arizona, ATTN: Director, Electronic Warfare Department
4	Chief, Research and Development Division, Office of the Chief Signal Officer, Department of the Army, Washington 25, D. C., ATTN: SIGEB
5	Commanding Officer, Signal Corps Electronic Research Unit, 9560th USASRU, P. O. Box 205, Mountain View, California
6	U. S. Atomic Energy Commission, 1901 Constitution Avenue, N. W., Washington 25, D. C., ATTN: Chief Librarian
7	Director, Central Intelligence Agency, 2430 E Street, N. W., Washington 25, D. C., ATTN: OCD
8	U. S. Army Research Liaison Officer, MIT-Lincoln Laboratory, Lexington 73, Massachusetts
9-18	Defense Documentation Center, Cameron Station, Alexandria, Virginia
19	Commander, Air Research and Development Command, Andrews Air Force Base, Washington 25, D. C., ATTN: SCEC, Hq.
20	Directorate of Research and Development, USAF, Washington 25, D. C., ATTN: Electronic Division
21-22	Hqs., Aeronautical Systems Division, Air Force Command, Wright-Patterson Air Force Base, Ohio, ATTN: WWAD
23	Hqs., Aeronautical Systems Division, Air Force Command, Wright-Patterson Air Force Base, Ohio, ATTN: WCLGL-7
24	Air Force Liaison Office, Hexagon, Fort Monmouth, New Jersey - For re-transmittal to - Packard Bell Electronics, P. O. Box 337, Newbury Park, California
25	Commander, Air Force Cambridge Research Center, L. G. Hanscom Field, Bedford, Massachusetts, ATTN: CROTLR-2
26-27	Commander, Rome Air Development Center, Griffiss Air Force Base, New York, ATTN: RCSSLD - For retransmittal to - Ohio State University Research Foundation
28	Commander, Air Proving Ground Center, ATTN: Adj/Technical Report Branch, Eglin Air Force Base, Florida
29	Chief, Bureau of Naval Weapons, Code RRR-E, Department of the Navy, Washington 25, D. C.

DISTRIBUTION LIST (Cont.)

Copy No.	
30	Chief of Naval Operations, EW Systems Branch, OP-35, Department of the Navy, Washington 25, D. C.
31	Chief, Bureau of Ships, Code 691C, Department of the Navy, Washington 25, D. C.
32	Chief, Bureau of Ships, Code 684, Department of the Navy, Washington 25, D. C.
33	Chief, Bureau of Naval Weapons, Code RAAV-33, Department of the Navy, Washington 25, D. C.
34	Commander, Naval Ordnance Test Station, Inyokern, China Lake, California, ATTN: Test Director - Code 30
35	Director, Naval Research Laboratory, Countermeasures Branch, Code 5430, Washington 25, D. C.
36	Director, Naval Research Laboratory, Washington 25, D. C., ATTN: Code 2021
37	Director, Air University Library, Maxwell Air Force Base, Alabama, ATTN: CR-4987
38	Commanding Officer - Director, U. S. Naval Electronics Laboratory, San Diego 52, California
39	Office of the Chief of Ordnance, Department of the Army, Washington 25, D.C., ATTN: ORDTU
40	Commanding Officer, U. S. Naval Ordnance Laboratory, Silver Spring 19, Maryland
41-42	Chief, U. S. Army Security Agency, Arlington Hall Station, Arlington 12, Virginia, ATTN: IADEV
43	President, U. S. Army Defense Board, Headquarters, Fort Bliss, Texas
44	President, U. S. Army Airborne and Electronics Board, Fort Bragg, North Carolina
45	U. S. Army Antiaircraft Artillery and Guided Missile School, Fort Bliss, Texas
46	Commander, USAF Security Service, San Antonio, Texas, ATTN: CLR
47	Chief, Naval Research, Department of the Navy, Washington 25, D. C., ATTN: Code 931
48	Commanding Officer, 52d U. S. Army Security Agency, Special Operations Command, Fort Huachuca, Arizona

DISTRIBUTION LIST (Cont.)

Copy No.

49	President, U. S. Army Security Agency Board, Arlington Hall Station, Arlington 12, Virginia
50	The Research Analysis Corporation, 6935 Arlington Rd., Bethesda 14, Maryland, ATTN: Librarian
51	Carlyle Barton Laboratory, The Johns Hopkins University, Charles and 34th Streets, Baltimore 18, Maryland
52	Stanford Electronics Laboratories, Stanford University, Stanford, California, ATTN: Applied Electronics Laboratory Document Library
53	HRB - Singer, Inc., Science Park, State College, Pennsylvania, ATTN: R. A. Evans, Manager, Technical Information Center
54	ITT Laboratories, 500 Washington Avenue, Nutley 10, New Jersey, ATTN: Mr. L. A. DeRosa, Div. R-15 Lab.
55	Director, USAF Project Rand, via Air Force Liaison Office, The Rand Corporation, 1700 Main Street, Santa Monica, California
56	Stanford Electronics Laboratories, Stanford University, Stanford, California, ATTN: Dr. R. C. Cumming
57	Stanford Research Institute, Menlo Park, California
58-59	Commanding Officer, U. S. Army Signal Missile Support Agency, White Sands Missile Range, New Mexico, ATTN: SIGWS-EW and SIGWS-FC
60	Commanding Officer, U. S. Naval Air Development Center, Johnsville, Pennsylvania, ATTN: Naval Air Development Center Library
61	Commanding Officer, U. S. Army Electronics Research and Development Laboratory, Fort Monmouth, New Jersey, ATTN: U. S. Marine Corps Liaison Office, Code AO-C
62	Director, Fort Monmouth Office, Communications-Electronics Combat Development Agency, Bldg. 410, Fort Monmouth, New Jersey
63-71	Commanding Officer, U. S. Army Electronics Research and Development Laboratory, Fort Monmouth, New Jersey ATTN: 1 Copy – Director of Research 1 Copy – Technical Documents Center ADT/E 1 Copy – Chief, Special Devices Branch, Electronic Warfare Div. 1 Copy – Chief, Advanced Techniques Branch, Electronic Warfare Div. 1 Copy – Chief, Jamming and Deception Branch, Electronic Warfare Div. 1 Copy – File Unit No. 2, Mail and Records, Electronic Warfare Div. 3 Cpys – Chief, Security Division (For retransmittal to - EJSM)

DISTRIBUTION LIST (Cont.)

Copy No.

72	Director, National Security Agency, Fort George G. Meade, Maryland, ATTN: TEC
73	Dr. B. F. Barton, Director, Cooley Electronics Laboratory, The University of Michigan, Ann Arbor, Michigan
74-97	Cooley Electronics Laboratory Project File, The University of Michigan, Ann Arbor, Michigan
98	Project File, The University of Michigan Office of Research Administration, Ann Arbor, Michigan
99	Bureau of Naval Weapons Representative, Lockheed Missiles and Space Co., P. O. Box 504, Sunnyvale, California - For forwarding to - Lockheed Aircraft Corp.
100	Lockheed Aircraft Corp., Technical Information Center, 3251 Hanover Street, Palo Alto, California

Above distribution is effected by Electronic Warfare Division, Surveillance Department, USAELRDL, Evans Area, Belmar, New Jersey. For further information contact Mr. I. O. Myers, Senior Scientist, Telephone 5961262

ERRATA

Technical Report No. 138

4853-18-T

Page 6 Equation 14a $\overline{\overline{A}}_{o_{out}}$ should read $\overline{A}_{o_{out}}$

Page 9 Equation 21 Delete vertical bar before "in|$\phi-\phi'$|"

Page 10 Line 3 - Equation should read:

$$\Phi^{(2)} = \left(H_1(r, K, \nu) + B \frac{K_n(\alpha_1 a)\, J_n(\alpha_2 r)}{J_n(\alpha_2 a)} \right) e^{\pm i n \phi} \cos \beta_m z$$

Page 14 Paragraph 2 $(k_i^2 - \beta_m^2)^{1\,2}$ should read $(k_i^2 - \beta_m^2)^{1/2}$

Page 16 Appendix I

Line 5 should read:

$$I_n(\beta_m r) \left[(K \mp \nu) n \int_r^a K_n(\beta_m r') I_n \left(\frac{\beta_m r'}{\sqrt{1+K}} \right) dr' + \frac{K \beta_m}{\sqrt{1+K}} \int_r^a K_n(\beta_m r') I_n \left(\frac{\beta_m r'}{\sqrt{1+K}} \right) r' \, dr' \right] \Bigg\}$$

Line 9 should read:

$$I_n(\beta_m r) \left[(\mp K - \nu) n \int_r^a K_n(\ m r') I_n \left(\frac{\beta_m r'}{\sqrt{1+K}} \right) dr' - \right.$$